BOLLETTINO DI GEOFISICA TEORICA ED APPLICATA VOL. XXXVII, N. 147 - SEPTEMBER 1995

M. FEDI [1] and A. RAPOLLA [2]

VERTICAL GRAVITY AND MAGNETIC SOUNDINGS : FORWARD PROBLEM FORMULATION AND DATA INVERSION

Abstract. A new method of interpreting gravity and magnetic anomalies is described. Unlike in the usual approaches, the data set consists of gravity values at different altitudes and the estimated model is a vertical density profile. Thus a new sounding method is defined, called vertical gravity, or magnetic sounding. In order to estimate the density model three methods are applied, all giving notable results. In particular, the " minimum length with inequality constraints" method seems particularly useful and, using a limited amount of "a priori" information, gives density models very close to several synthetically generated density distributions. A major feature of the proposed method is that significant results are obtained without resorting to other geophysical or drilling data.

INTRODUCTION

Geophysical data can be interpreted using very different approaches, depending mainly on the nature of the mathematical equations relating the measured data to the unknown physical parameters, such as "gravity-density", "arrival times of seismic waves-seismic velocity" and so on. However, such equations, defining the so-called "forward problem", cannot be solved completely using just the data; additional information is required.

This involves making some reasonable assumptions on the distribution of the investigated physical parameter. For example, when gravity data are measured along horizontal profiles, the interpretation can only be done by considering a 2-D or a 2.5-D forward problem formulation, i.e. by assuming that the density distribution does not vary along the direction normal to the profile. Similar assumptions are made for seismic or electrical data.

Thus, even if from a general point of view the physical parameters are 3-D functions, say μ (x,y,z), we are rarely able to obtain a complete description of them. In this respect there is a major difference between electrical or seismic data and potential field ones. The first are essentially interpreted using vertical distribution models of resistivity and seismic velocity. However, gravity data measured at some topographic surface cannot be inverted directly in terms of vertical density variations ϱ (z), and the same is true for magnetic susceptibility. In fact, it is well known that an infinite number of density distributions at varying depths can equally well solve the inverse gravity problem (Grant and West, 1965). This lack of uniqueness is normally overcome by introducing information from direct observation (drilling holes) or other geophysical data. Another way of deducing some depth estimates of density and magnetization is to make strong geometrical and/or statistical assumptions on their distributions (Spector and Grant, 1970; Reid et al., 1990; Roest et al., 1992). However only limited information can be estimated, for example, the depth to the top of anomaly sources, and often with a non-negligible error.

Manuscript received, December 23, 1993; accepted, August 19, 1994.

[1] Università di Lecce, Dipartimento di Scienza dei Materiali, via per Arnesano, 73100 Lecce, Italy.

[2] Università di Napoli, Dipartimento di Geofisica e Vulcanologia, Largo San Marcellino 10, 80138 Napoli, Italy.

So, we can conclude that, even if a large number of different methods has been proposed to interpreted gravity and magnetic data, any of them cannot be used to directly infer the distribution of density and magnetization with depth.

This paper deals specifically with this problem, and a new way of interpreting potential field data is proposed. Our aim is to show that very significant results can be achieved using nothing but the information related to potential field data.

The basic idea is that the vertical density or magnetic distribution can be deduced from the gravity field known at different altitudes. The feasibility of the method will be shown for the case of a horizontally-finite and vertically-layered source, that is a 1-D model with end effects. A paper in preparation will deal with more complex sources, which can be used to interpret actual gravity anomalies.

THE VERTICAL GRAVITY SOUNDING

In this section we deal with the inverse problem of determining the depth distribution of density or magnetization by inversion of gravity or magnetic data. Since we are describing methods applicable in a similar way to both these types of data, we will refer, for simplicity, only to the gravity case.

Let us consider the following discrete set of N measured points

$$P(\vec{r}_k)=P(x_0, y_0, z_k) \qquad k=1, \ldots, N.$$

At these points, the gravity field due to a mass distribution of density $\varrho(\vec{r})$ in a volume V can be defined as

$$g(z_k)=\gamma \int_V \varrho(\vec{r}) \frac{z-z_k}{|\vec{r}-\vec{r}_k|^3} dv, \tag{1}$$

where γ is the gravitational constant.

If density varies only with the vertical coordinate

$$\varrho(\vec{r})=\varrho(z),$$

the integral (1) simplifies to

$$g(z_k)=\gamma \int_V \varrho(z) \frac{z-z_k}{|\vec{r}-\vec{r}_k|^3} dv. \tag{2}$$

Eqn (2) defines the 1-D forward problem of a continuous unknown function $\varrho(z)$ linearly related to the measured gravity data. Diversely from 1-D electrical or seismic problems, the horizontal extension of the volume in eqn. (1) is finite and has to be fixed before inverting. However, several papers (Blakely and Simpson, 1986; Roest et al., 1992) show techniques to estimate quite precisely this prism parameter from gravity-tranformed anomalies, such as horizontal derivatives and analytical signals.

In this paper we will use discrete inverse theory, so that the following forward problem will be defined:

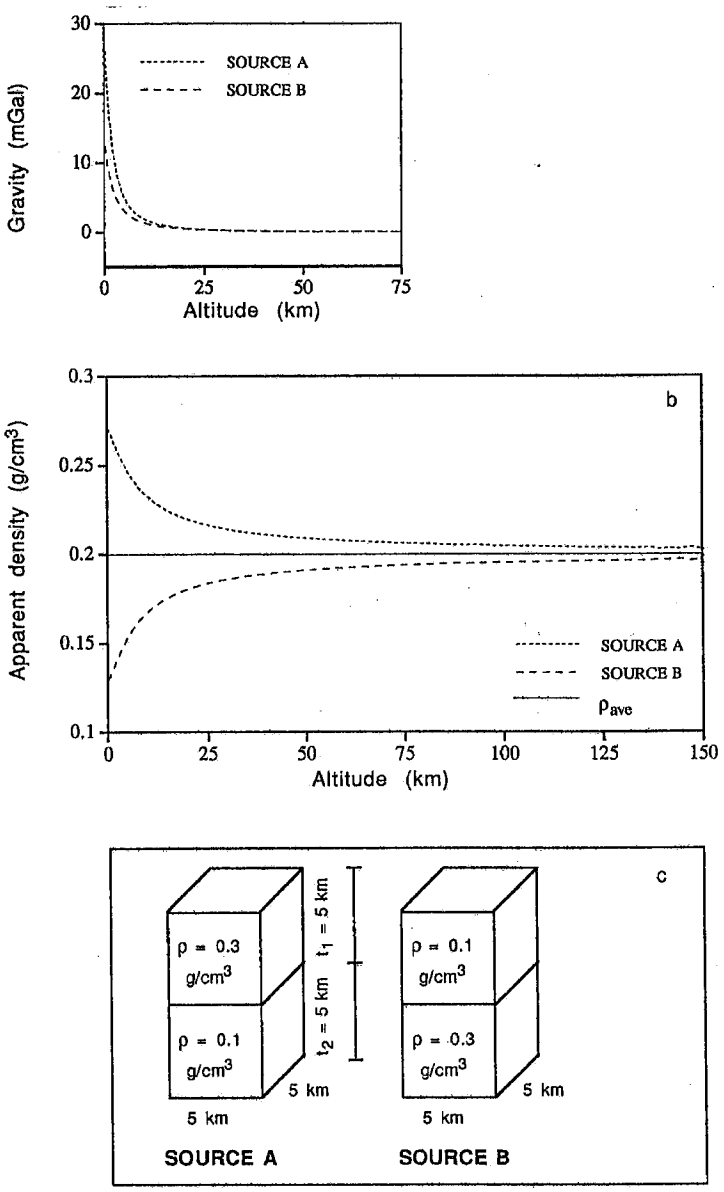

Fig. 1 — Vertical gravity (a) and apparent density (b) profiles for two-layer sources (c) with a more dense (Source A) and a less dense (Source B) upper layer. Note that the apparent density shapes allow the two cases to be clearly distinguished.

$$g(z_k) = \sum_{j=1}^{M} \varrho_j \; G_j(z_k) \qquad k=\{1, \ldots, N\}, \tag{3}$$

where

$$G_j(z_k) = \gamma \int_{V_j} \frac{z - z_k}{|\vec{r} - \vec{r}_k|^3} \, dv$$

is the unit-density contribute due to the jth prismatic layer and

$$\sum_{j=1}^{M} V_j = V. \tag{4}$$

Note that there are two possible ways to obtain the N values of eqn. (3). Obviously, the first is by measuring the gravity field at the corresponding points. However, if a gravity map is available at some altitude z_k, either upward or downward continued data can be computed using efficient numerical methods.

Eqn. (3) defines the forward problem of a "gravity vertical sounding" (G.V.S.). In matrix notations eqn. (3) can be written as

$$g_k = \sum_{j=1}^{M} G_{kj}\, \varrho_j \qquad k=\{1, \ldots, N\},\ j=\{1, \ldots, M\}. \tag{5}$$

In this paper, starting from this equation, the inverse problem of estimating the M-vector ϱ from the N-vector data **g** and the theoretical NxM kernel matrix **G** will be discussed . More particularly, three different techniques will be proposed to solve this problem.

THE TWO-LAYER CASE USING APPARENT DENSITIES

In this section, the very simple case of two-layers is described (Fig. 1). Eqn. (5) can then be written as

$$g_k = G_{1k}\, \varrho_1 + G_{2k}\, \varrho_2 \qquad k=1, \ldots, N. \tag{6}$$

For a given volume V, let us define the apparent density $<\varrho\ (z_k)>$ such that

$$\langle \varrho(z_k) \rangle = \frac{g(z_k)}{G(z_k)} = \frac{\int_V \varrho(z)\, \frac{z-z_k}{|\vec{r}-\vec{r}_k|^3}\, dv}{\int_V \frac{z-z_k}{|\vec{r}-\vec{r}_k|^3}\, dv}. \tag{7}$$

As shown in eqn. (7), $<\varrho(z_k)>$ is a weighted average of ϱ (z) with the weights

$$\frac{z-z_k}{|\vec{r}-\vec{r}_k|^3}.$$

From eqns. (6) and (7), we find for apparent densities

$$<\varrho>_k = (h_1)_k\, \varrho_1 + (h_2)_k\, \varrho_2, \tag{8}$$

where $(h_1)_k$ and $(h_2)_k$ are the weighting functions

$$(h_1)_k = \frac{G_{1k}}{G_k} \qquad (h_2)_k = \frac{G_{2k}}{G_k}, \tag{9}$$

and G_{1k}, G_{2k}, G_k are the unit-density gravity values at points P (0, 0, z_k), referred to the volumes V_1, V_2, V. Let us now consider the case of two sources (Fig. 1c) having the same

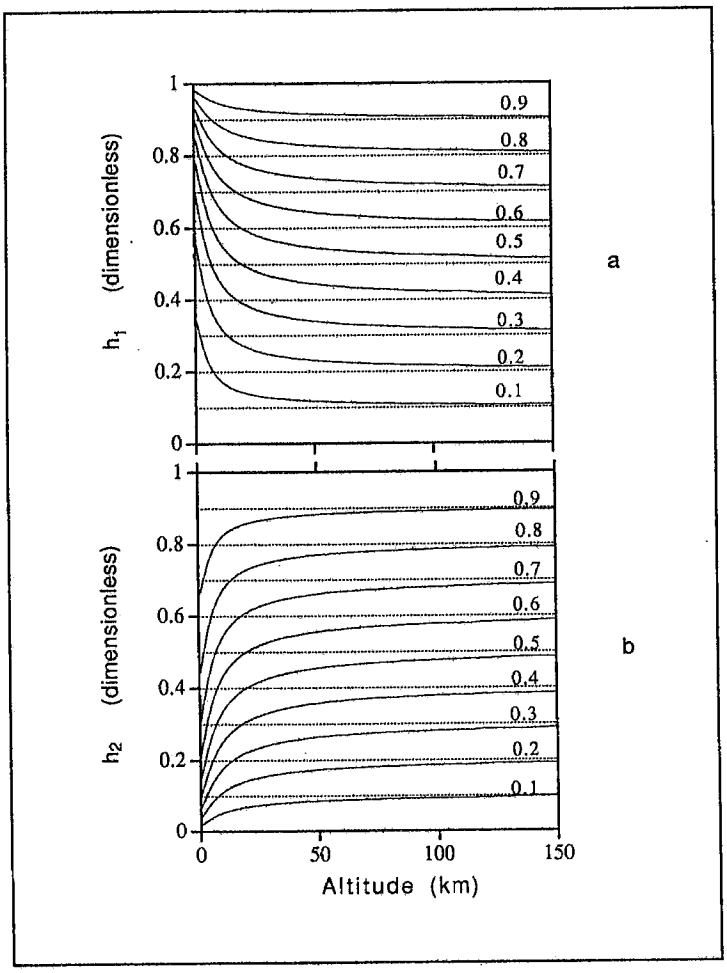

Fig. 2 — Parametric curves of the weighting functions h_1 (a) and h_2 (b). The parameters are, respectively, t_1/t and t_2/t. Note that, for large vertical distances, the curves tend to the asymptote defined by their own parameter value (dashed lines).

dimensions, but with the first layer respectively denser (Source A) or less dense than the second (Source B). Also if a slower decay rate for Source B is seen (Fig. 1a), it is difficult to distinguish the two cases from the shape itself of the profiles. Diversely, the apparent density curves (Fig. 1b) are strongly characterized by the two density distributions: a decreasing function of the altitude in the first case, and an increasing one in the second case. This clearly show that the information contained in the vertical profiles of gravity is strongly related to $\varrho(z)$.

It is important to note that at large vertical distances the apparent density tends to the asymptote corresponding to the weighted average of the layer densities. In fact, in this case

$$\frac{z-z_k}{|\vec{r}-\vec{r}_k|^3} \simeq -\frac{1}{z_k^2} \quad , \tag{10}$$

and the apparent density in eqn. (7) becomes

$$\lim_{z_k \to \infty} \langle \varrho(z_k) \rangle = \frac{\varrho_1 V_1 + \varrho_2 V_2}{V_1 + V_2} = \frac{M}{V} \quad ,$$

where M is the total source mass.

As regards the weighting functions, similarly note that for a prism of dimensions a, b, t

$$\int_V \frac{z-z_k}{|\vec{r}-\vec{r}_k|^3} dv \simeq \frac{abt}{z_k^2} ,$$

so that we can readily find

$$\lim_{z_k \to \infty} [h_1(z_k)] = \frac{t_1}{t} ,$$

$$\lim_{z_k \to \infty} [h_2(z_k)] = \frac{t_2}{t} ,$$

where t_1 and t_2 are the thicknesses of the upper and lower layers respectively.

Thus, for large distances such functions approximate the asymptote defined by a very simple geometrical factor related to the layer thickness. In Fig. 2 the parametric curves of $(h_1)_k$ and $(h_2)_k$ are shown, with the ratios t_1/t (Fig. 2a) and t_2/t (Fig. 2b) as parameters.

Another remarkable property of the weighting functions follows from their definition itself (eqn. (9)):

$$(h_1)_k + (h_2)_k = 1 .$$

Using this equation, eqn. (9) can be rewritten as

$$\langle \varrho \rangle_k = (\varrho_1 - \varrho_2)(h_1)_k + \varrho_2 . \tag{11}$$

Thus, it suffices to know two values of $\langle \varrho \rangle_k$ to determine uniquely $(h_1)_k$. In fact, since

$$\begin{aligned} \langle \varrho \rangle_{k1} &= (\varrho_1 - \varrho_2)(h_1)_{k1} + \varrho_2 , \\ \langle \varrho \rangle_{k2} &= (\varrho_1 - \varrho_2)(h_1)_{k2} + \varrho_2 , \end{aligned} \tag{12}$$

we have also

$$\langle \varrho \rangle_{k1} - \langle \varrho \rangle_{k2} = (\varrho_1 - \varrho_2)[(h_1)_{k1} - (h_1)_{k2}].$$

So, at every other point z_k we can define a normalized density function R, such that

$$R_{(z_{k1}, z_{k2}, z_k)} = \frac{\langle \varrho \rangle_k - \langle \varrho \rangle_{k2}}{\langle \varrho \rangle_{k1} - \langle \varrho \rangle_{k2}} = \frac{(h_1)_k - (h_1)_{k2}}{(h_1)_{k1} - (h_1)_{k2}} .$$

This function does not depend on the layer densities and thus, using the third member of the above equation, t_1 can be theoretically computed from the parametric curves of the weighting functions. The two-layer set of parametric curves of R can be used to interpret any apparent density vertical profile of a two-layer source. In Fig. 3 two examples of normalization are shown. The first is for $z_{k1} = 0$ and $z_{k2} = 36$ km (Fig. 3a). The curves are clearly separated, but a stronger effect can be obtained with a different choice of points: $z_{k1} = 11$ km and $z_{k2} = 18$ km (Fig. 3b). Thus, a possible technique to interpret a vertical gravity profile is based on the following steps: (a) compute the apparent densities (see Fig. 1b); (b) normalize them; (c) compare the normalized apparent densities to the corresponding theoretical R curves, such as those of Fig. 3, and estimate the ratio t_1/t. The two values of normalization should be selected in order to obtain a sufficient curve separation. Applying the technique to the vertical profile of Fig. 1a, source A, a normalized profile is obtained exactly matching the parametric curve for $t_1/t = 0.5$. From this ratio, the depth interface can be readily computed. Finally, it is a simple matter to solve the system of two eqns. (12) and compute the layer densities ϱ_1 and ϱ_2.

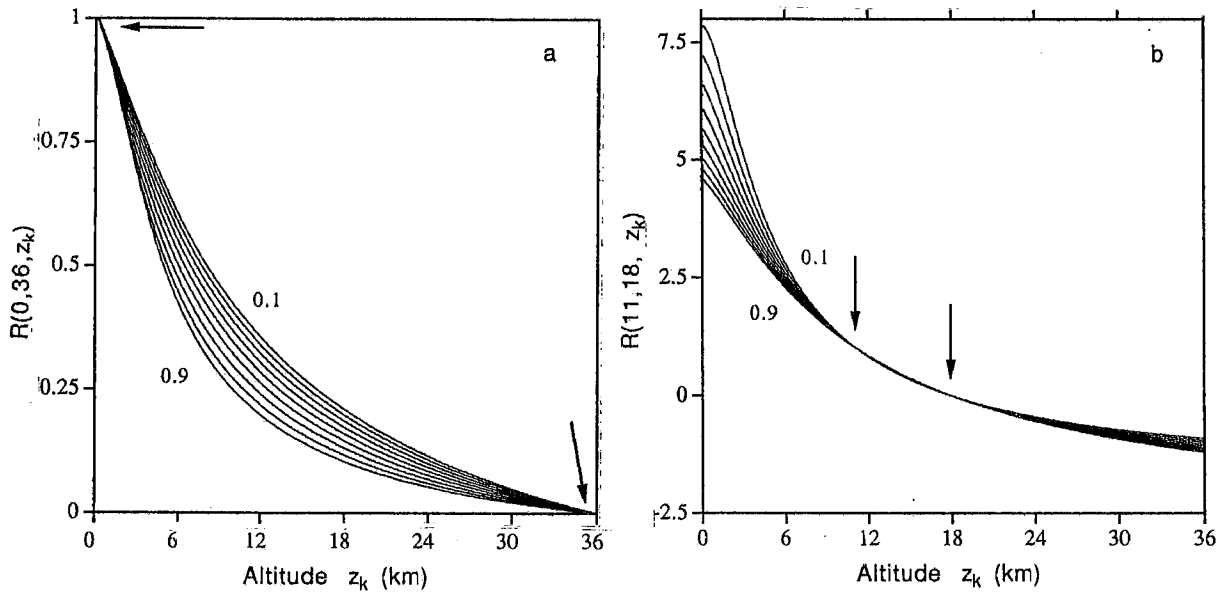

Fig. 3 — Normalized apparent density curves for $z_{k1}=0$ and $z_{k2}=36$ km (a) and $z_{k1}=11$ and $z_{k2}=18$ km (b). The curves parameters is the ratio t_1/t. Since these curves do not depend on the layer densities, they can be used to estimate the upper layer thickness from a function R computed by gravity data (see text).

The technique described in this section is simple and allows a two-layer case to be easily solved. However, a certain amount of "a priori" information is needed, that is the source volume and its depth. So, even if the depth to the source top can often be sufficiently deduced by several methods (for example: Spector and Grant, 1970), a greater uncertainty generally affects the depth to the source bottom estimation, and thus the volume. Furthermore, the extension to the more realistic case of more than two layers is relatively complex.

Thus, other techniques will be described in the next section, which can resolve the multi-layer case and require much less "a priori" information.

THE MULTI-LAYER CASE USING THE SVD TECHNIQUE

In this paper two different inverse theory methods will be used to solve the linear system (5). It is well known that solving a linear system is not straightforward, due to critical properties of the kernel matrix **G**. Instability of solutions, for example, arises when the system is ill-conditioned; that is when small perturbations of the data vector lead to very different model solutions. This property is of obvious relevance, because experimental data are always affected by errors. The non-uniqueness of undetermined systems and the trade-off between model resolution and variance are well described in the basic papers of Backus and Gilbert (1967; 1968; 1970) and Parker (1977). See also Tarantola (1987) and Menke (1984) for a more complete description of inverse problem theory.

Since geophysical inverse problems are very often poorly-determined, methods that can isolate the part of the solution well determined by the data are very useful. To this end, a technique named Singular Value Decomposition (S.V.D) can be used (Lanczos, 1961; Jackson, 1972). For forward problems such as that in eqn. (5),

$$\boldsymbol{g}=\boldsymbol{G}\varrho\ , \tag{13}$$

the SVD technique consists in decomposing **G** in the following way:

$$G = U\Lambda V^T , \tag{14}$$

where U is a NxN matrix formed by eigenvectors $[u_1 , ..., u_N]$ of GG^T ; V is a MxM matrix formed by eigenvectors $[v_1 , ..., v_M]$ of G^TG ; Λ is the diagonal NxM eigenvalue matrix defined from

$$\begin{bmatrix} O & G \\ G^T & O \end{bmatrix} \begin{bmatrix} u_i \\ v_i \end{bmatrix} = \lambda_i \begin{bmatrix} u_i \\ v_i \end{bmatrix} ,$$

where $\mathbf{0}$ is a zero matrix.

Normally, eigenvalues are ordered decreasingly with the null ones last, for $i \geq p$, where: $p \leq \min (M,N)$.

In this case, eqn. (14) can be written

$$G = U_p \Lambda_p V_p^T , \tag{15}$$

where Λ_p is the corresponding pxp eigenvalue matrix, while $\mathbf{U}_p$ and $\mathbf{V}_p$ are the Nxp and Mxp submatrices of $\mathbf{U}$ and $\mathbf{V}$.

It is now a simple matter to show that the solution of eqn. (13), ϱ, is given simply by

$$\varrho = V_p \Lambda_p^{-1} U_p^T g . \tag{16}$$

However, in order to have a significant solution, the degree of conditioning of $\mathbf{G}$ should be also evaluated, which can be done using the ratio between the maximum (λ_1) and minimum (λ_p) eigenvalues. Ill-conditioning arises when λ_p is very small with respect to λ_1 .

In this case, a large variance will characterize the solution ϱ, since it is proportional to $(\Lambda_p)^{-2}$. To reduce this problem several techniques can be adopted. The simplest is to consider a new index value $q \leq p$ with the eigenvalue λ_q not as small as λ_p , and define three new submatrices Λ_q , $\mathbf{U}_q$ and $\mathbf{V}_q$ with this reduced dimension.

The corresponding solution

$$\varrho = V_q \Lambda_q^{-1} U_q^T g \tag{17}$$

will now have a lower resolution, but a more acceptable variance or, in other words, the well-determined part of the solution has been found and separated from the unstable part.

In order to apply the S.V.D technique to the inverse problem (13), synthetic vertical profiles with five different density distributions were generated. The first density distribution (VGS-A) corresponds to a prismatic source of constant density $\varrho = 0.3$ g/cm^3, depth to the top $z_1 = 3.5$ km, depth to the bottom $z_2 = 8$ km and with a square horizontal section of side $w = 5$ km. The vertical profile (vector $\mathbf{g}$) consisted of 25 points sampled with a 0.3 km step, from 0 to 7.5 km (Fig. 4a).

We used a model of 100 layers of equal thickness, from 0 to 16 km. Note that with the 1-D inversion the total layer thickness should be chosen as large as necessary to contain any non-zero density layer. The SVD solution ϱ shown in Fig. 4b was obtained. The actual density distribution is substantially approximated by the density model found, but some widening and a slight instability at shallow depths are present (q is 44% p). Trying to reduce instability with a smaller q-dimension is not satisfactory, because of the corresponding lack in resolution.

However, a better result can be obtained using SVD and a stacking procedure, consisting in taking the average values of a set of solutions obtained using different layer thicknesses. The stacking was applied to the ϱ solutions relative to 200 different 5-layer models (Fig. 4c),

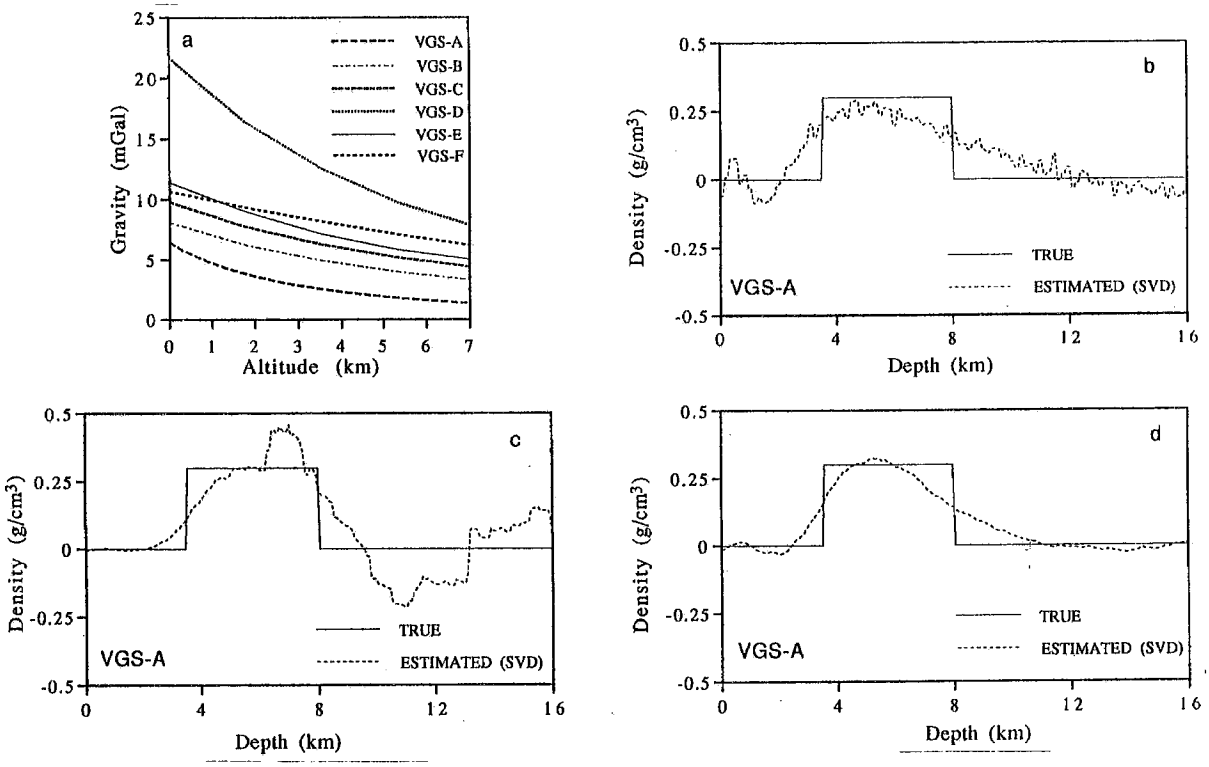

Fig. 4 — The vertical gravity profile VGS-A (a) corresponds to the box-car density distribution of Figs 4b-4d (solid line). The modelled density distributions (dashed lines) are obtained using SVD technique for a 100 layer model (Fig. 4b) and with a stacking technique (see text: Figs 4c and 4d).

and to 200 20-layer models (Fig. 4d). For each of the 200 models the layer thicknesses were determined by a generator algorithm of random uniform deviates (Press et al., 1992). These figures show that, once a optimum layer number is determined, in this case M = 20, the stacked solution is more stable and close to the true density distribution than the 100-layer model of Fig. 4b.

The next VGS were performed on more complex density distributions, such as the discontinuous five-step one of the VGS-B, shown in Fig. 5a. The region of non-zero density is quite well identified, but it can be noted that SVD does not allow the central low density region to be well resolved. However, for a similar distribution of greater extension (VGS-C, Fig. 5b), the estimated densities are in good agreement with the true ones. Similarly, if a smoothed oscillating density distribution is considered (VGS-D, Fig. 5c) a better result is also obtained for the low density region. The last vertical gravity sounding was made for a ramp density distribution (VGS-E, Fig. 5d) and the estimated densities are again in good agreement with the synthetic model.

The above examples show that SVD applied to vertical gravity soundings gives significant results. The standard deviation of the differences between true and modelled data was always small, of the order of 10^{-3} mGal, while that between true and estimated densities was of the order of 10^{-2} g/cm^3. However, the best resolved models arise for smoothed density distributions, while some widening appears for discontinuous ones. This is unavoidable, since the first spectral components are smoothed functions themselves. So, due to the regularization procedure that suppress the unstable and high-frequency components of the solution, sharp density variations can no longer be modelled.

In the next section, a more powerful technique will be described, allowing a very good resolution to be obtained.

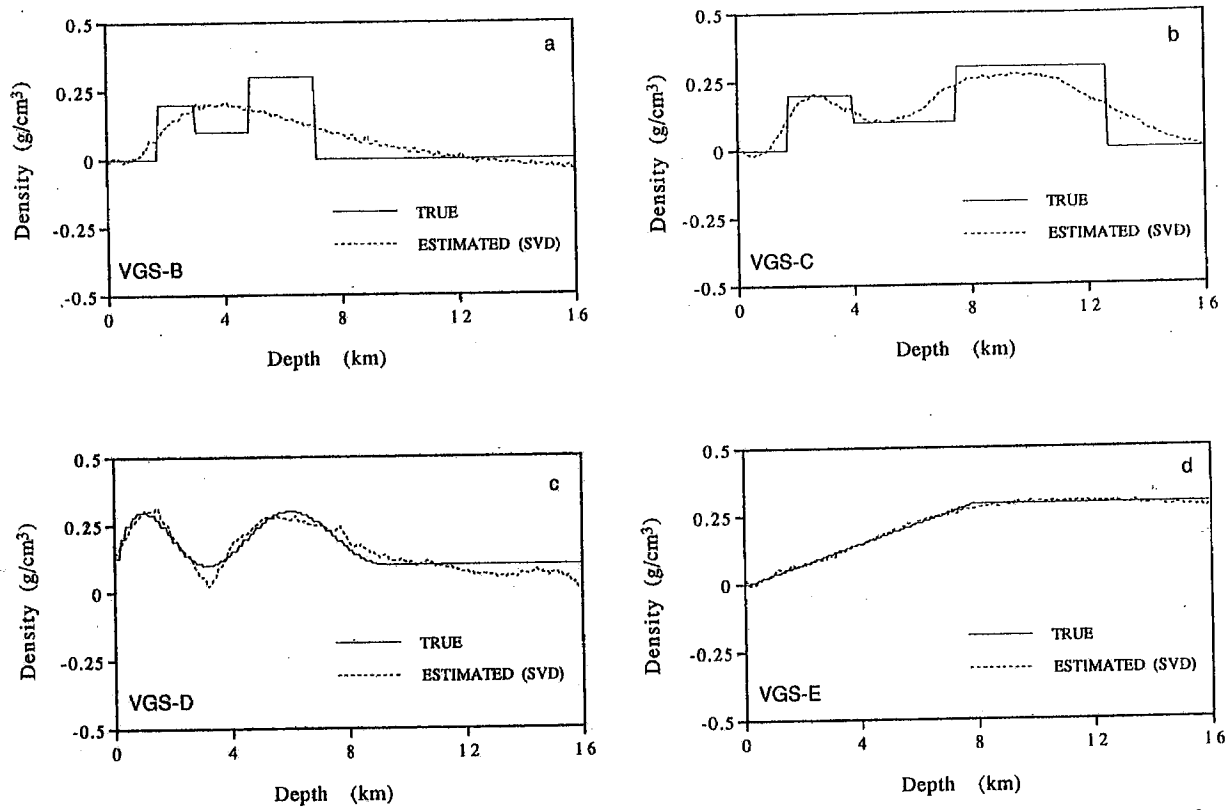

Fig. 5 — The SVD inversion results are shown for four different density distributions (solid lines). See Fig. 4a for the corresponding gravity profiles. Note that the 5-step model (a) is not well resolved in the central low-density part. Better results are obtained in the other cases (b; c; d).

THE MULTI-LAYER CASE USING THE IML TECHNIQUE

A technique of estimating densities from VGS is here described, which produces stable solutions without losing high-frequency solution components. The technique, which we call "Minimum Length with Inequality constraints" or IML, deals with undetermined linear problems, such as that of eqn. (13). Its model estimates are given by the solution having the minimum Euclidean length, or L_2 norm:

$$\varrho^T\varrho = \sum_{i=1}^{M} \varrho_i^2 = \|\varrho\|_2^2 \,, \tag{18a}$$

and which also satisfies some set of linear inequality constraints

$$\boldsymbol{F}\,\varrho \geq \boldsymbol{h} \tag{18b}$$

where **F** is an NxM matrix and **h** is an N-vector.

If eqn. (18b) assumes the particular form

$$\boldsymbol{G}\varrho = \boldsymbol{d} \,,$$

the model estimate is the well known "minimum length" solution for undetermined problems (Menke, 1984)

$$\varrho^{est} = \boldsymbol{G}^T[\boldsymbol{G}\boldsymbol{G}^T]^{-1}\boldsymbol{d} \,.$$

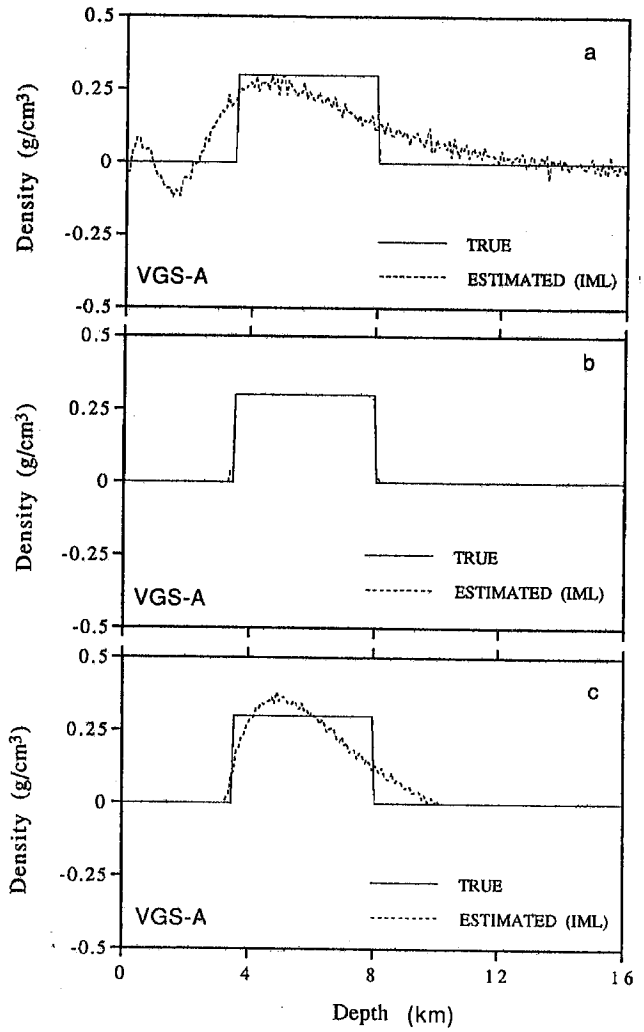

Fig. 6 — Discontinuous density distributions, such as the box-car one (solid line), are better estimated using the IML method (see text). Fairly well resolved models are obtained, if just non-negative densities are allowed (b; c). For wider bounds (a) a similar result is obtained to that of the SVD technique (Fig. 4).

However, the general constraint formulation of eqn. (18b) is more useful, since it allows "a priori" information to be easily added to the problem. For example, in actual interpretation problems, density can be very reasonably bounded by some extremal values, and we shall show that this kind of "a priori" information can help to find very significant and stable solutions to the system (13).

A very useful technique to solve the I. L. M. problem is based on the Kuhn-Tucker theorem (for instance: Fiacco and Mc Cormick, 1968) which indicates the conditions that should be satisfied by the solution. In practice, the constraints of eqn. (18b) define a volume in the model-space of feasible solutions. If constraints are consistent, this volume is non-zero and there is at least one solution satisfying both conditions of eqs. (18). Following a technique described in Menke (1984) the minimum-length problem is first transformed into the non-negative least squares problem:

$$\textit{minimize:} \quad e=\|\boldsymbol{f}-\boldsymbol{E}\boldsymbol{u}\|_2 \quad \textit{subject to:} \quad \boldsymbol{u}\geq 0 \ , \tag{19}$$

where $\mathbf{u}$ is an N vector, and the (M+1)xN matrix $\mathbf{E}$ and the M+1 vector $\mathbf{f}$ are given by

$$\mathbf{E}=\begin{bmatrix} \mathbf{F}^T \\ \boldsymbol{h}^T \end{bmatrix} , \boldsymbol{f}=\begin{bmatrix} \mathbf{0} \\ \boldsymbol{1} \end{bmatrix} .$$

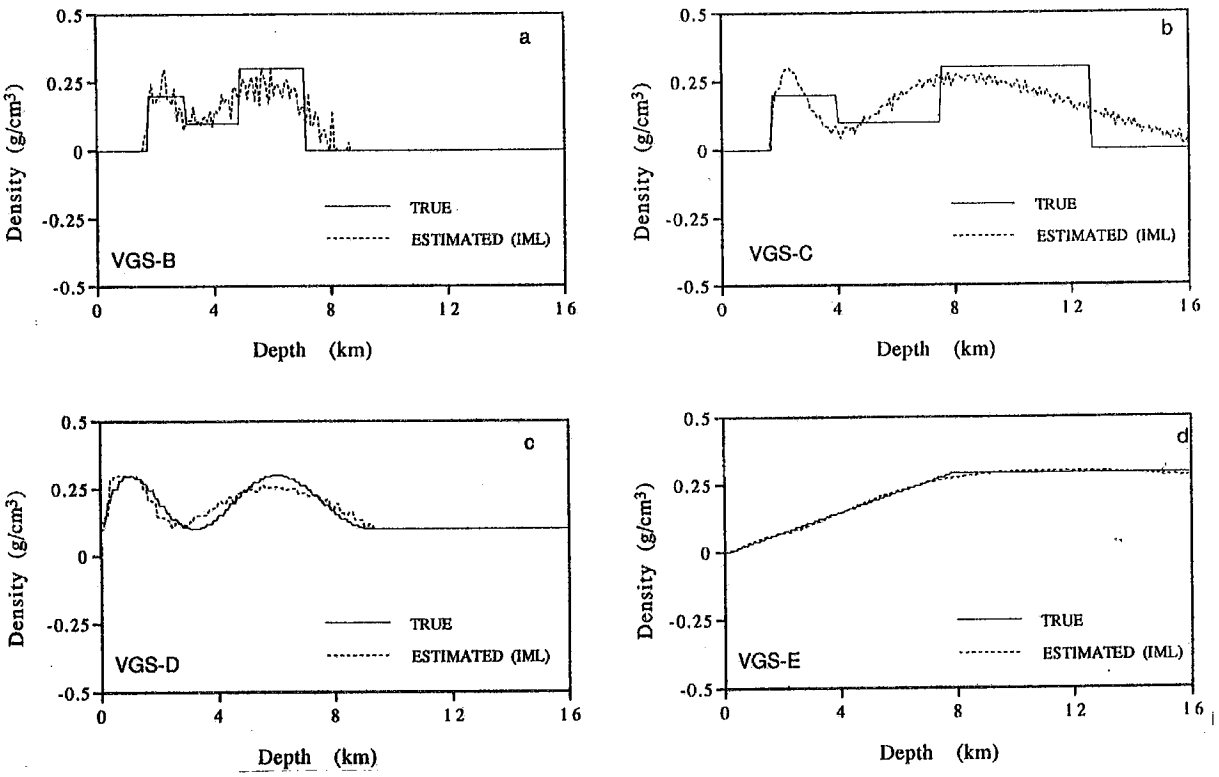

Fig. 7 — The same density distributions of Fig. 5 (solid lines) are estimated using the IML method. By comparison with the SVD interpretations, a better resolved result is obtained for the 5-step model (a), while similar results come out for the other distributions.

As an intermediate step, this problem is solved using the Kuhn-Tucker theorem. An iterative cycle is built, where a feasible model $\mathbf{u_k}$ is perturbed to decrease the error $\mathbf{e}$ and maintain $\mathbf{u_{k+1}} = \mathbf{u_k} + \mathbf{du}$ feasible. The final solution $\mathbf{u^{est}} = \mathbf{u_k}$ is found when the direction of decreasing error would force $\mathbf{u_{k+1}}$ to be unfeasible.

Finally, the solution of problem (18) is found from

$$(\varrho^{est})_i = e_i / e_{M+1} \qquad i=(1,\ldots, M) \; . \tag{20}$$

Let us now define the constraint inequalities which will be used in this paper. They are based essentially on two points:

(a) the unknown density vector ϱ has to satisfy the forward problem (3), slightly modified in order take into account experimental errors $\delta\mathbf{d}$:

$$\boldsymbol{d} - \delta\boldsymbol{d} \leq \boldsymbol{G}\varrho \leq \boldsymbol{d} + \delta\boldsymbol{d} \; ; \tag{21a}$$

(b) instability and/or unrealistic density estimates can be avoided by opportunely bounding the density vector:

$$\varrho_L \leq \varrho_i \leq \varrho_H \qquad i=(1,\ldots, M) \; , \tag{21b}$$

where ϱ_L and ϱ_H have to be chosen in some broad sense, when only gravity data are available. On the other hand, density constraints can be made as strong as desired, if drilling or other geophysical data are available.

As with SVD, synthetic vertical profiles with five different density distributions were generated and then inverted using the IML algorithm. A standard deviation between true and modelled

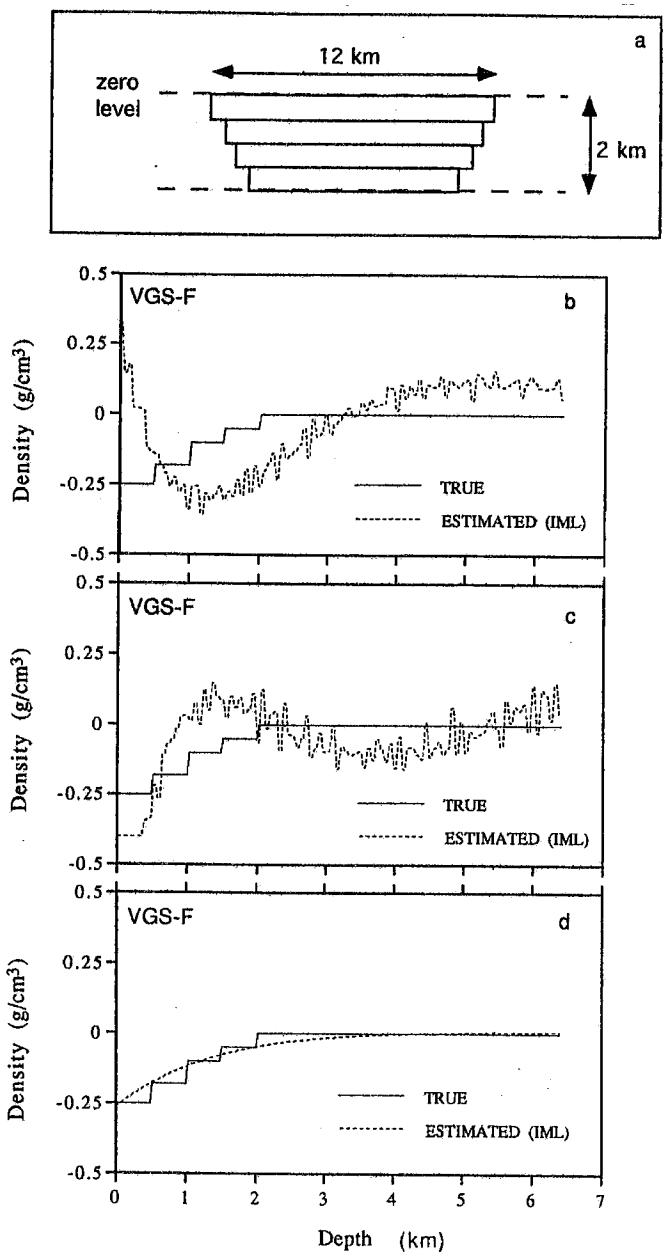

Fig. 8 — Sources having a variable layer side w(z) can also be analyzed (a) with vertical gravity soundings (see text and Fig. 4a). Using an equivalent-prism source, a good estimation of the actual density distribution (solid line) is obtained for an optimal side w* = 11.2 km (d), while two class of unstable solutions arise for larger (w = 11.8 km: b) and smaller sides (w = 11.0 km: c). A 10% error data does not affect the result.

data similar to that obtained with the SVD method was obtained, while a better result, 10^{-3} g/cm^3, was obtained with respect to the modelled densities. The first VGS was done using the case A source, with 100 layers and the following constraints:

$$(\delta d)_i = 1 \times 10^{-5}\ mGal \qquad i=(1,\ldots, M)\ ,$$

$$\varrho_L = -0.3\ g/cm^3; \qquad \varrho_H = 0.3\ g/cm^3.$$

A somewhat similar result to that of SVD (Fig. 6a) can be observed. However, an impressively better inversion can be done by changing the density bounds in order to consider only positive values:

$$\varrho_L = 0 \ g/cm^3; \qquad \varrho_H = 0.3 \ g/cm^3 \ . \tag{22}$$

In this case, (Fig. 6b) any slight instability disappears and the discontinuous density distribution is perfectly interpreted. This result is very remarkable, when compared with any other existing interpretative method. Note that the depths to the top and bottom of a prismatic source can be safely estimated, without resorting to any independent information (seismic and/or other). Furthermore, the interpretation is not limited to only these two parameters, but gives excellent estimates at any depth level.

In order to test the method with other choices of the bounding densities, another IML inversion was done using a higher upper bound ($\varrho_H = 0.5$ g/cm^3). Fig.6c shows that a significant result is obtained in this case too. The depth to the top is again very precisely estimated, while some widening appears at the bottom. On the other hand, the main observation is that even using such a large upper bound, densities very close to the true ones are estimated.

The other VGS, shown in Fig. 7a, also gives satisfying models. If we compare the IML and SVD results, the main difference again is in their resolution power for discontinuous density distributions, such as that of VGS-B (Fig. 7a). In fact, the IML model shows a well pronounced low-density central zone, apart from some high-frequency noise. The more smoothed density distributions of the soundings VGS-C, VGS-D and VGS-E give, however, similar results with both methods (Figs. 7b, 7c and 7d).

Up to now, error-free data have been considered. However, even when adding an error as large as 10%, a good-quality result is still obtained. A final example will illustrate this. Let us consider a layered source with a depth increasing density (Fig. 8) and with a decreasing horizontal side for each layer. Since the side extensions are unknown, an equivalent prismatic source, with some horizontal dimension w, is used to invert the corresponding VGS. A data error of 10% was also considered and the density bounds were

$$\varrho_L = -0.4 \ g/cm^3; \qquad \varrho_H = 0.4 \ g/cm^3.$$

Fig. 8 shows that unstable solutions are generated (Figs 8b; c), unless an optimal equivalent-prism side is found, which is $w^* = 11.2$ km (Fig. 8d). Note that this value of w can easily be found since: a) for greater values ($w = 11.8$ km, Fig. 8b) and lower ones ($w = 11.0$ km, Fig. 8c) we obtain two density profile groups of symmetrical shape with respect the x-axis; b) for $w = w^*$ the density profiles of the two groups converge to the actual solution.

CONCLUSIONS

We have defined and described a method of 1-D modelling as a powerful tool to interpret gravity or magnetic anomalies. Vertical gravity soundings can give a complete description of the density distribution with depth and allow a new approach to considering the interpretation of potential field data. In fact, the traditionally undetermined parameters of a source, such as depths to the bottom and top, appear now well determined by the variation of gravity with altitude. The concept itself of "isolated source" no longer has meaning with this approach, since all the layered space along the direction of the sounding is explored and the "source" as here appears nothing but that a sub-set of non-zero density layers over the whole depth extension. Two techniques, SVD and IML, have given satisfying interpretations for a number of synthetically generated density distributions, the second appearing more powerful. We are now working on a generalization of the technique to more complex 3-D cases.

REFERENCES

Backus G. and Gilbert F.; 1967: *Numerical applications of a formalism for geophysical inverse problems.* Geophys. J. R. Astr. Soc. **13**, 247-276.

Backus G. and Gilbert F.; 1968: *The resolving power of gross earth data.* Geophys. J. R. Astr. Soc. **16**, 169-205.

Backus G. and Gilbert F.; 1970: *Uniqueness in the inversion of inaccurate gross Earth data.* Phil. Trans. R. Soc. London Ser. A, **266**, 123-192.

Blakely R.J. and Simpson R.W.; 1986: *Approximating edges of source bodies from magnetic or gravity anomalies.* Geophysics, **51**, 1494-1498.

Fiacco A.V. and McCormick G.P.; 1968: *Nonlinear programming: sequential unconstrained minimization techniques.* John Wiley and Sons, New York, 251 pp.

Grant F.S. and West G.F.; 1965: *Interpretation theory in applied geophysics.* Mc Graw-Hill, New York, pp. 583.

Jackson D.D.; 1972: *Interpretation of inaccurate, insufficient and inconsistent data.* Geophys. J.R.A.S. **28**, 97-109.

Lanczos C.; 1961: *Linear differential operators.* Van Nostrand-Reinhold, Princeton, 564 pp.

Menke W.; 1984: *Geophysical data analysis: discrete inverse theory.* Academic Press, Inc., 260 pp.

Parker R.L.; 1977: *Understanding inverse theory.* Ann. Rev. E.Pl.Sc, **5**, 35-64.

Press W.H., Flannery B.P., Teukolsky S.A. and Vetterling W.T.; 1989: *Numerical recipes.* Cambridge University Press. Cambridge, 702 pp.

Reid A.B., Allsop J.M., Granser H., Millett A. and Somerton I.W.; 1990: *Magnetic interpretation in 3-D using Euler deconvolution.* Geophysics, **55**, 80-91.

Roest W.R., Verhoef J. and Pilkington M.; 1992: *Magnetic interpretation using 3D analytic signal.* Geophysics, **57**, 116-125.

Spector A. and Grant S.; 1970: *Statistical models for interpreting aeromagnetic data.* Geophys., **35**, 293-302.

Tarantola A.; 1987: *Inverse problem theory.* Elsevier. Amsterdam, 613 pp.